International Journal of Sediment Research 32 (2017) 442–451

Contents lists available at ScienceDirect

International Journal of Sediment Research

journal homepage: www.elsevier.com/locate/ijsrc

Original Research

Phosphorus fractions and sorption dynamics in the sediments of two Ca-SO_4 water reservoirs in the central Argentine Andes

José Gabriel León [a,b,*], Fernando Luis Pedrozo [c], Pedro Félix Temporetti [c]

[a] Instituto Argentino de Nivología, Glaciología, y Ciencias Ambientales (IANIGLA), CCT Mendoza. Av. R. Leal s/n, 5500 Mendoza, Argentina
[b] Departamento General de Irrigación, Gobierno de Mendoza, España y Barcala, 5500 Mendoza, Argentina
[c] Instituto de Investigaciones en Biodiversidad y Medio Ambiente (INIBIOMA), CONICET - Universidad Nacional del Comahue, Quintral 1250, 8400 S. C. de Bariloche, Argentina

ARTICLE INFO

Article history:
Received 14 April 2016
Received in revised form
24 January 2017
Accepted 8 March 2017
Available online 16 March 2017

Keywords:
Reservoir
Internal load
Phosphorus binding
Calcareous watershed
Southern Central Andes

ABSTRACT

Phosphorus (P) fractionation and sorption behavior were studied in the sediments of two calcium-sulfate (Ca-SO_4: Ca^{2+} 170 mg L^{-1}; SO_4^{2-} 400 mg L^{-1}) water reservoirs in the southern central Argentine Andes - El Carrizal Reservoir (ECR),which stratifies in summer and El Nihuil Reservoir (ENR),which is vertically mixed throughout the year. Sediment size classes reflected the lithology of both basins and the reservoirs relative location: ECR (downstream from a valley adjacent to a mountain environment) had higher clay proportions while the sand fraction was more important in ENR (just next to a mountain environment). In both reservoirs, the chemical composition revealed low alteration and calcium enrichment. Total P content was relatively high (1.1 – 1.6 mg P kg^{-1} dry weight) as expected from the contribution of marine formations. P fractionation was dominated by Ca-P (ECR, 69% and ENR, 63%) followed by organic-P (23%) in summer-anoxic ECR and by iron/aluminum (Fe/Al)-P (27%) in oxic ENR. Batch experiments showed that sorption behavior in ECR had a typical Langmuir isotherm plot while in ENR that model fitted only at low dissolved P values (< 5 mg P L^{-1}) and co-precipitation evidence was observed at higher P concentrations. It is proposed that lower Fe/Al-P content in anoxic (ECR) *vs*. oxic (ENR) sediments results from the P released from iron-bound phosphorus due to sulfate reduction-ferrous sulfide formation in an anoxic environment. This condition should enable ECR sediments to adsorb P into fresh oxidized iron, and ENR sediments to co-precipitate P with calcium due to Fe/Al-P saturation, as observed in batch experiments. This paper constitutes the first description of phosphorus content and dynamics in reservoir sediments in arid central western Argentina, where water sulfate concentrations are naturally high due to basin lithology.

1. Introduction

In aquatic systems, phosphorus (P) cycling through the sediment compartment is a significant term in the mass balance of this vital element; therefore, quantifying the sediment P content and speciation constitutes the initial step to understanding the P cycle in aquatic environments, and getting to estimate its relative importance in the eutrophication process (Golterman, 2004). The flux of P from and towards the water column and the physical, chemical, and biological factors controlling it are usually investigated by analyzing the sediment granulometry, mineralogy, and P fractionation and sorption behavior (Limousin et al., 2007; Lukkari et al., 2007). In the pelagic environment, and depending on the physical and chemical conditions therein, equilibrium is established between the dissolved P and the P attached to particles (and forming a structural part of those); and similarly, the P input/output balance in the lake bottom is controlled by the biogeochemical conditions at the sediment-water interface (Boström et al., 1988; Lu et al., 2016). In highly productive systems, the bottom physical and chemical conditions cause a series of elements (P among them) to be released from sediments to the water column promoting eutrophication and other water quality problems (Sinke, 1992; Wetzel, 2001).

In reservoirs, bottom sediments mainly originate from rock erosion in the fluvial catchment, and P content and fractionation depend on basin-scale factors such as watershed geology, hydrometeorological conditions, and anthropic inputs (Smal et al., 2013), and also on autochthonous processes such as photosynthesis and

* Corresponding author at: Cooperativa de Obras y Servicios Públicos Ltda. Bv. H. Irigoyen y Chaco, 5862 Villa del Dique, Argentina..
E-mail address: leondecba@yahoo.com.ar (J.G. León).

http://dx.doi.org/10.1016/j.ijsrc.2017.03.002
1001-6279/

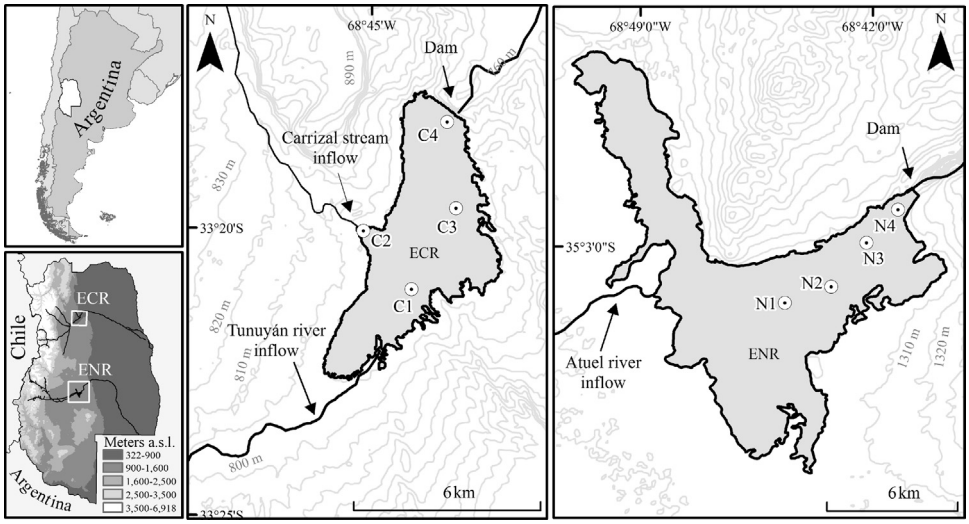

Fig. 1. Sampling site locations in El Carrizal Reservoir (ECR) and El Nihuil reservoir (ENR).

respiration (Wetzel, 2001). P transformations in sediments depend on several parameters related to water quality (such as thermal stratification, pH, redox potential, and concentrations of iron, aluminum, sulfate, and calcium) and to dam operation (Keitel et al., 2016). Also, these factors influence the P sorption capacity of the sediments, which is strongly related to water chemistry (*e.g.*, calcium and sulfate concentrations) and sediment granulometry (especially to finer fractions [$< 4\ \mu m$]), organic matter content, and iron (Fe) and aluminum (Al) oxy(hydr)oxides and calcium carbonate ($CaCO_3$) concentrations (Berg et al., 2004; Golterman, 2004; Smal et al., 2013; Wang et al., 2006).

Sediment P content and chemical distribution are usually studied by extraction schemes such as that proposed by Hieltjes and Lijklema (1980). These methods consist of sequential extractions using different solvents to transfer P from solid to liquid phase, where P is quantified (Sahuquillo et al., 2002). On the other hand, P sorption mechanisms in sediment are usually studied through empirical models that describe the characteristics of sorption processes in sediments such, as Freundlich and Langmuir isotherms (Limousin et al., 2007).

Phosphorus fractionation and sorption dynamics in aquatic sediments have been extensively studied in coastal sediments (Cong et al., 2014), and in lakes and reservoirs in granitic and calcareous basins (Borgnino et al. 2006a, 2006b; Dittrich et al., 2013; Hupfer et al., 2009; Temporetti & Pedrozo, 2000), but little information has been reported from freshwater lakes having naturally high sulfate concentrations (Temporetti et al., 2013). In anoxic sediments, sulfate (SO_4^{2-}) may be used as electron acceptor in organic matter oxidation by sulfate-reducing bacteria producing H_2S, which combines with Fe to form FeS making P release from iron oxy(hydr)oxides (Chen et al., 2016; Yu et al., 2015), and, thus, affecting the eutrophication process. Sulfate pollution has been indicated as a growing environmental problem in aquatic environments (Baldwin & Mitchell, 2012); in this regard, the reservoirs studied in this paper may constitute natural experiments to assess the effect of high sulfate concentration on geochemical processes acting upon P binding and speciation in sediments.

The aims of this study are to characterize the bottom sediments in two Ca-SO_4 water reservoirs differing in their thermal regime (summer stratification *vs.* year-round mixing), and to assess their ability to remove dissolved P in relation to physical and chemical features of sediment, and to water quality parameters.

Table 1.
Physical and chemical features of El Carrizal Reservoir (ECR) and El Nihuil Reservoir (ENR) (Baffico et al., 2007; León, 2013). Water transparency (*i.e.* Secchi disk depth) and chlorophyll ***a*** correspond to the epilimnion and chemical composition to the hypolimnion (annual average).

		ECR	ENR
Surface area	(km^2)	31	108
Volume	(hm^3)	320	236
Mean depth	(m)	10.3	2.2
Hydraulic residence time	(years)	0.3	0.2
Secchi disk depth	(m)	1.4	> 3.0
pH		**8.1**	**8.3**
Conductivity	($\mu S\ cm^{-1}$)	1265	1283
Dissolved oxygen	($mg\ L^{-1}$)	6.8	7.0
Calcium (Ca^{2+})	($mg\ L^{-1}$)	170	170
Magnesium (Mg^{2+})	($mg\ L^{-1}$)	14	23
Sodium (Na^+)	($mg\ L^{-1}$)	54	116
Potassium (K^+)	($mg\ L^{-1}$)	4	6
Sulfate (SO_4^{2-})	($mg\ L^{-1}$)	404	410
Bicarbonate (HCO_3^-)	($mg\ L^{-1}$)	109	116
Chloride (Cl^-)	($mg\ L^{-1}$)	64	147
Total P	($\mu g\ L^{-1}$)	193	45
Total N	($\mu g\ L^{-1}$)	512	133
Soluble Reactive P (SRP)	($\mu g\ L^{-1}$)	42	25
Nitrate + Nitrite ($N\text{-}NO_3 + N\text{-}NO_2$)	($\mu g\ L^{-1}$)	303	76
Ammonium ($N\text{-}NH_4$)	($\mu g\ L^{-1}$)	50	9
Chlorophyll ***a***	($\mu g\ L^{-1}$)	7.0	3.0

2. Methods

2.1. Study area

El Carrizal Reservoir (ECR) and El Nihuil Reservoir (ENR) are located in the alluvial plains of the arid southern Central Andes of Argentina (Fig. 1). The geology of their upstream catchments consists of Miocene volcanic rocks, and Mesozoic and Paleogene sedimentary and magmatic formations on top of Late Paleozoic/Triassic magmatic sequences (Kay et al., 2004). Sedimentary formations include sandstones, black shales, carbonates, gypsum and halite (Ramos et al., 2010). The water chemistry in both ECR and ENR is dominated by Ca^{2+} and $SO_4^{2-}$and by sodium (Na^+) and chloride (Cl^-) (Table 1) from evaporite dissolution and carbonate weathering in the headwaters (León & Pedrozo, 2015; Manzur et al., 2006). Additionally, ENR receives even higher Na^+ and Cl^- loads due to hydrothermal activity in the upper basin (Nullo et al., 2005). As the tributaries of both reservoirs are mainly fed by snow and glacier melt in the Andes highlands (Masiokas et al., 2010),

inflow discharge and solids load are highly seasonal (León & Pedrozo, 2015).

Both reservoirs were primarily built for irrigation purposes and hydropower generation. The ECR (mean depth 10 m; area 30 km^2) is located in the middle basin of the Tunuyán River, which constitutes its main tributary (1100 hm^3 y^{-1}). A second smaller inflow is the Carrizal Stream (30 hm^3 y^{-1}), which is fed by nitrogen-enriched irrigation drainage (dissolved inorganic N *ca.* 5 mg L^{-1}). The ECR is located at 785 m asl and is deep enough to allow the development of a stratifying limnetic zone where primary production is dominated by phytoplankton (León et al., 2016). ENR is located at 1325 m asl and is the first of a series of reservoirs in the middle basin of the Atuel River (1110 hm^3 y^{-1}). The ENR water column is mixed year-round and its morphometry corresponds to that of a shallow lake (mean depth 3 m; area 75 km^2) having a macrophyte coverage > 50% comprised by *Potamogeton pectinatus* and *Myriophyllum aquaticum* in the limnetic sector and *Chara* sp. dominating the riverine area (Peralta & León, 2006). In the northwestern part of the reservoir there is a long and narrow lobe which corresponds to a temporarily connected shallow wetland (mean depth 1 m) which receives water from the reservoir at maximum water level. This wetland does not actively interact with the reservoir and its water is more concentrated due to evaporation (Peralta & León, 2006).

2.2. Sampling and processing

Four samples were collected along each reservoir longitudinal axis from the river inflow to the dam (Thornton et al., 1990), in ENR in January 2007 and in ECR in June 2009 (Fig. 1). Samples were taken with an Ekman-Birge dredge, stored in plastic bags and conserved in cold and dark conditions until analysis. Sediment pH was measured *in situ* (Thermo-Orion pH/ORP meter 920 A). Samples consisted in the bulk material from the upper *ca.* 0.2 m portion of the sediments extracted with the dredge corresponding to the last 3–4 years for ECR and 5–7 years for ENR (EVARSA, 2006, 2013). All samples were homogenized and dried at 60 °C for 72 hours, then gently powdered in ceramic mortar and sieved through 500 μm mesh sieves (ASTM No. 35) to remove the coarser less-reactive fraction. Each sample of dry sediment was analyzed for grain size distribution, chemical and mineralogical constitutions, P fractionation, and P sorption. All analyses were performed in triplicate.

2.3. Granulometry, chemical and mineralogical composition

The grain size distribution was determined by laser diffraction (Mastersizer 2000, Optical Unit Hydro 2000-MU, Malvern Instruments Ltd). For each sample, the percentage composition in the size range from 0.42 to 831.76 μm was obtained and then classified according to the modified Wentworth scale (clay < 4 μm < silt < 63 μm < sand [Golterman, 2004]).

Sediment total phosphorus (TP) was determined by digesting samples at 440 °C with concentrated sulfuric acid (H_2SO_4) and hydrogen peroxide (H_2O_2) 30% (Carter & Gregorich, 2006) in a Hach Digesdahl® Digestion Apparatus, followed by soluble reactive P (SRP) determination (Murphy & Riley, 1962). The total nitrogen (TN) and total carbon (TC) proportions were determined in a Thermo® Flash EA 1112 automatic analyzer. Organic matter content was estimated by mass loss on ignition (LOI) after combustion for 2 hours at 550 °C.

The elemental composition of the bulk sample was determined by SEM-EDS microanalysis (Philips515-EDAXGenesis 2000).The mineralogical composition was determined by X-ray diffraction (XRD) analysis in the bulk sample. The XRD pattern of each sample was obtained by using a Philips PW 1701/01, Cu-Kα radiation at 40 kV and 30 mA, 2θ range 5–65°, 0.03° step size.

2.4. Phosphorus fractionation

Phosphorus fractions were determined according to Hieltjes and Lijklema (1980), discriminating: the labile fraction (labile-P), extracted with 1 M ammonium chloride (NH_4Cl); Fe- and Al-bound fraction (Fe/Al-P), extracted with 0.1 M sodium hydroxide (NaOH); and calcium-bound fraction (Ca-P), extracted with hydrochloric acid (HCl) 0.5 M. The organic matter-bound P fraction (org-P) was calculated from the difference between total P (TP) and the sum of the fractions determined.

2.5. Phosphorus sorption

Batch experiments were done by measuring dissolved P in a mixture of dried sediment and a set of increasing P concentration solutions (0, 1.7, 2.7, 3.7, 4.5, 5.5, 8.5, 10.0, 15.0 and 20.0 mg P L^{-1}prepared from a 1000 mg phosphate (PO_4) L^{-1} Merck Certipur® solution). Sediment aliquots (*ca.* 0.2 g) were put in centrifuge tubes (50 mL) filled with P solution (10 mL) and placed in the dark at room temperature (20 °C) for 48 hours with periodic mixing (2 hours in orbital shaker). The supernatant was filtered (0.45 μm) and analyzed for P (Murphy & Riley, 1962). The maximum P adsorption capacity in the sediment (P_{max}, mg g^{-1}) was estimated by using the linearized Langmuir equation (Langmuir, 1997):

$$1/P_{ads} = 1/(K_L \cdot P_{max}) \cdot P_{dis} + (1/P_{max})$$

where P_{ads} (mg g^{-1}) is the net phosphorus adsorbed in sediment estimated from dissolved P mass difference between the initial and final solution after 48 hours, K_L (L mg^{-1}) is a constant relating P binding energy to sediment, P_{max} is the maximum sorption capacity and P_{dis} (mg L^{-1}) is the P concentration remaining in solution after 48 hours (Sposito, 2008). The equilibrium P concentration (EPC_0, *i.e.* the dissolved P concentration in the solution at which net P sorption is zero) was estimated as the *x* intercept of the fitted simple linear regression of P_{ads} *vs.* P_{dis} for $P_{dis} < 5$ mgL^{-1}; and the native adsorbed P (NAP, *i.e.* the P concentration adsorbed in sediments previous to P sorption experiences), as the *y* intercept (Lin et al., 2009; Zhou et al., 2005). Dissolved P in the treatment with no added P (*i.e.* deionized water) was considered as desorpted P (P_{des})

2.6. Statistical analyses

Dataset comparisons and association between variables were estimated by Kruskal-Wallis analysis and the Spearman rank order correlation coefficient (R_S), respectively. Principal Component Analysis (PCA) was done to analyze relations between considered variables and sampling sites in both reservoirs. All statistical analyses were performed using the Infostat software (Di Rienzo et al., 2013).

3. Results

Sediments characteristics are summarized in Table 2. In both reservoirs, grain size distribution was poorly-sorted sandy muds. In the ECR, the silt fraction had the greater proportion (70%) followed by the clay fraction (20%); while in the ENR, silt and sand fractions shared the dominance (40%). The clay fraction was homogeneously distributed along the longitudinal axis in both ECR and ENR. The sediments' chemical composition in the two reservoirs was characterized by calcium enrichment (Fig. 2). Mean pH was slightly alkaline in ECR sediments (8.0) and circumneutral in

Table 2
Sediment extraction depth, pH, grain size distribution, and chemical composition in the El Carrizal Reservoir (ECR) and El Nihuil Reservoir (ENR). Grain size classes: clay, < 4 μm; silt, 4 - 63 μm; sand, > 63 μm. LOI stands for loss on ignition, d.w. means dry weight, and wt% means percent by weight. Variables marked with * indicate a significant difference between reservoirs ($p < 0.05$, $n = 4$. Kruskal-Wallis test). See text for variables reference.

		ECR				ENR			
		C1	C2	C3	C4	N1	N2	N3	N4
Depth	(m)	0.8	1.5	20.0	30.0	2.7	11.0	4.5	17.0
pH*		8.0	7.8	8.1	8.0	7.2	7.2	7.0	7.5
Clay	(%)	19	19	22	21	17	22	23	12
Silt	(%)	76	73	57	45	43	48	50	41
Sand	(%)	5	8	21	34	40	30	27	47
Na	(wt%)	2.7	1.4	1.7	1.9	1.9	1.9	2.3	2.0
Mg	(wt%)	2.0	2.2	1.9	2.1	1.7	2.1	1.8	1.7
Al	(wt%)	10.1	10.2	8.9	9.4	9.2	10.5	10.2	8.7
Silicon (Si)	(wt%)	27.7	27.4	27.1	27.8	26.0	27.1	27.9	29.6
K	(wt%)	2.0	2.1	1.8	1.6	1.8	1.8	1.8	1.6
Ca	(wt%)	4.7	5.6	8.8	6.9	10.2	5.5	4.5	5.5
Titanium (Ti)	(wt%)	0.4	0.4	0.3	0.3	0.3	0.4	0.3	0.2
Fe	(wt%)	3.6	3.8	3.3	3.3	3.1	3.9	4.0	3.3
LOI	(%)	3.4	6.3	5.2	5.5	5.8	7.3	6.4	10.0
Total Carbon (C)	(%)	1.6	2.6	3.4	3.3	5.1	4.6	3.0	4.1
Total N*	(%)	0.01	0.14	0.12	0.14	0.19	0.21	0.18	0.35
Total P*	(mg g^{-1} d.w.)	1.3	0.9	1.1	1.2	1.4	1.7	1.8	1.4
Labile-P*	(mg g^{-1} d.w.)	0.02	0.02	0.02	0.03	0.05	0.07	0.08	0.10
Fe/Al-P*	(mg g^{-1} d.w.)	0.04	0.04	0.05	0.09	0.24	0.49	0.51	0.50
Ca-P	(mg g^{-1} d.w.)	0.95	0.66	0.80	0.83	1.10	1.02	1.14	0.79
Organic-P*	(mg g^{-1} d.w.)	0.30	0.24	0.25	0.29	0.09	0.11	0.12	0.02

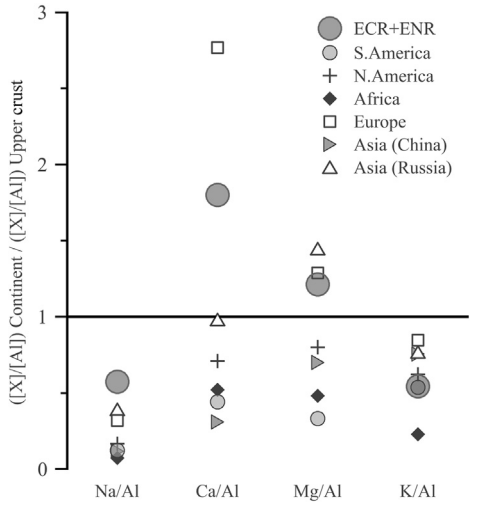

Fig. 2. Enrichment factors with respect to Upper Crust composition for major elements in sediments from the El Carrizal and El Nihuil reservoirs (ECR + ENR) and for suspended particulate matter in rivers from Africa, Europe, South America, North America, Asia (China), and Asia (Russia). Modified from Viers et al. (2009).

ENR sediments (7.2) (Table 2). In ECR, loss on ignition (LOI), total carbon (TC), TN, and TP ranged between 3.4–6.3%, 1.6–3.4%, 0.01–0.14%, and 0.9–1.3 mg g^{-1} dry weight (d.w.), respectively (Table 2); while in the ENR these constituents varied between 5.8–10.0%, 3.0–5.1%, 0.18–0.35%, and 1.4–1.8 mg g^{-1} d.w., respectively (Table 2).The average values of pH, TN, TP, labile-P, Fe/Al-P, and org-P significantly differed between reservoirs ($p < 0.05$, $n = 4$); pH and org-P were higher in the ECR while TN, TP, labile-P, and Fe/Al-P concentrations were higher in the ENR (Table 2 and Fig. 3).

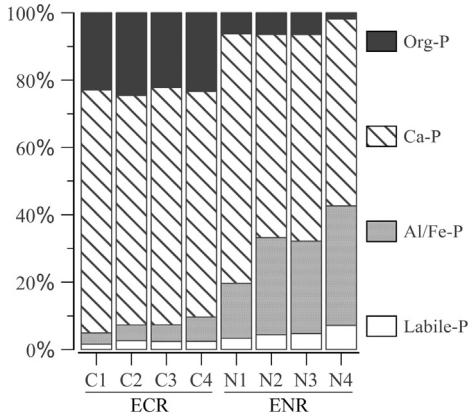

Fig. 3. Phosphorus fractions in sediments at sampling sites in El Carrizal Reservoir (ECR) and El Nihuil Reservoir (ENR).

The element ratio (Table 2) was Si > Al > Ca > Fe > Na-Mg > Ti in both reservoirs.

Mineralogical analyses (Table 3) reflected calcium richness. The sum of calcium carbonates and phosphates accounted for 14%, and the largest proportion of silicate minerals corresponded to Ca-plagioclase (29%). In all samples, the proportion of compounds considered easily weatherable was high (Pyroxene, Ca-plagioclase, carbonates, and phosphates: *ca.* 50%), while the more stable minerals had a lesser contribution, (K-feldspar, micas, and clays: *ca.* 30%). The content of P-bearing minerals was relatively high and it mainly consisted of Ca-phosphates and hydrated Al and Fe phosphates (11% and 3%, respectively).

The P-Ca fraction had the highest proportion in both reservoirs (Fig. 3) and did not differ between them (mean 63% of TP in the ENR and 69% of TP in the ECR). The rest of P fractions showed differences between the two waterbodies. The ENR had the higher P-Fe/Al (mean 27% of TP) and P-Labile (average 5% of TP) fractions, while the ECR had higher P-Org (mean 23% of TP) and lower P-Fe/Al (mean 5% of TP).

The results of P sorption experiments are shown in Fig. 4. The ECR data fitted the Langmuir model (Fig. 4a) as the increments of P_{ads} had a linear growing phase (up to *ca.* 5 mg L^{-1}) that flattened at higher P_{dis}. Isotherms in the ENR fitted the Langmuir model (Fig. 4b) for $P_{dis} < 3$ mg $L^{-1}$and deviated from it at higher concentrations; after the linear growing phase, the isotherm turned back on itself with decreasing P_{dis} and increasing P_{ads}, and then resumed the linear growth. P_{max} and the P binding constant K_L were estimated using positive values of P_{ads} (adsorption) from the linearized Langmuir isotherm for the ECR, and only the first phase of the isotherm was considered (*i.e.* P_{dis} from 0.2 to 2.5 mg L^{-1}) for the ENR (Table 4). The steeper slope of the ENR isotherm suggests a higher P retention capacity when compared to the ECR. Accordingly, higher P_{max} values were recorded in the ENR (0.579–2.181 mg g^{-1} d.w.) than in the ECR (0.200–0.358 mg g^{-1} d.w.). The average value of K_L was similar in both reservoirs (4.4 and 4.5 L mg^{-1} for the ECR and ENR, respectively); however, this constant relating P binding energy to sediment tended to display higher values at sites having finer granulometry. The NAP concentration accounted for 0.7–1.1% of TP and was lower in the ECR than in the ENR. The estimated EPC_0 at every site was always higher than the average SRP concentration in the overlying water (Tables 1 and 4). The phosphorus desorption (P_{des}: *i.e.* the final [P_{dis}] in the treatment with no added P) averaged 0.006 and 0.003 mg g^{-1} d.w. in the ECR and ENR, respectively (Table 4).

The relations between P fractions and physical and chemical parameters are shown in Table 5. The LOI was directly associated to TN as expected from the fact that both variables are related to

Table 3
Mineral species identified by X-ray diffraction in the sediments of the El Carrizal Reservoir (ECR) and El Nihuil Reservoir (ENR) and semi quantitative content values.

Compound name	Mineral group	Chemical formula	Composition per site (%)							
			ECR				ENR			
			C1	C2	C3	C4	N1	N2	N3	N4
Calcite	Carbonate	$CaCO_3$	1		4	5	2	2	1	1
Calcite magnesian	Carbonate	$(Mg\text{-}Ca)CO_3$	2		2	4	1	1	1	1
Monetite	Phosphate	$CaHPO_4$	3	13	4	3	6	7	7	6
Brushite	Phosphate	$CaHPO_4(H_2O)_2$	2	3	3	1	2	2	1	2
Anapaite	Phosphate	$Ca_2Fe(PO_4)_2(H_2O)_4$	2	3	2	2	4	3	3	3
Vivianite	Phosphate	$Fe_3(PO_4)_2(H_2O)_8$	1	1	3	4	4	1	1	1
Metavariscite	Phosphate	$Al(PO_4)(H_2O)_2$	1	2	1	1	1	1	1	1
Pyroxene	Pyroxene	$Mg_2\ Si_2\ O_6$	3	6	3	3	3	3	3	4
Diopside	Pyroxene	$CaMg(SiO_3)_2$	2	2	2	2	2	2	2	2
Anorthite	Plagioclase	$(Ca_{0.96}Na_{0.04})(Al_{1.96}Si_{0.04})Si_2O_8$	8	10	9	7	12	12	10	10
Bytownite	Plagioclase	$Ca_{0.86}\ Na_{0.14}\ (Al_{1.94}\ Si_{2.06}\ O_8)$	8	9	7	6	9	10	10	9
Labradorite	Plagioclase	$Ca_{0.64}Na_{0.35}(Al_{1.63}Si_{2.37}O_8)$	10	9	9	8	12	12	13	12
Andesine	Plagioclase	$Na_{0.685}Ca_{0.347(}(Al_{1.46}Si_{2.54}O_8)$	8	9	8	6	10	11	12	11
Albite	Plagioclase	$Na(AlSi_3O_8)$	7	5	6	5	8	8	9	9
Sanidine	K-feldspar	$K(AlSi_3O_8)$	5	4	3	4	3	3	3	4
Orthoclase	K-feldspar	$(K_{0.93}Na_{0.06}Ca_{0.01}Ba_{0.01})(AlSi_3O_8)$	3	4	3	2	2	3	3	3
Biotite	Mica	$KMg_3AlSi_3O_{10}OHF$	4	5	4	3	2	3	3	3
Muscovite	Mica	$KAl_{2.2}(Si_3Al)_{0.98}O_{10}((OH)_{1.7}O_{0.3})$	7	5	7	7	7	7	7	6
Kaolinite	Clay	$Al_4(OH)_8(Si_4O_{10})$	1	3	2	2	3	3	2	2
Illite-montmorillonite	Clay	$KAl_4(Si,Al)_8O_{10}(OH)_4 \cdot 4H_2O$	21	5	19	24	6	7	7	11

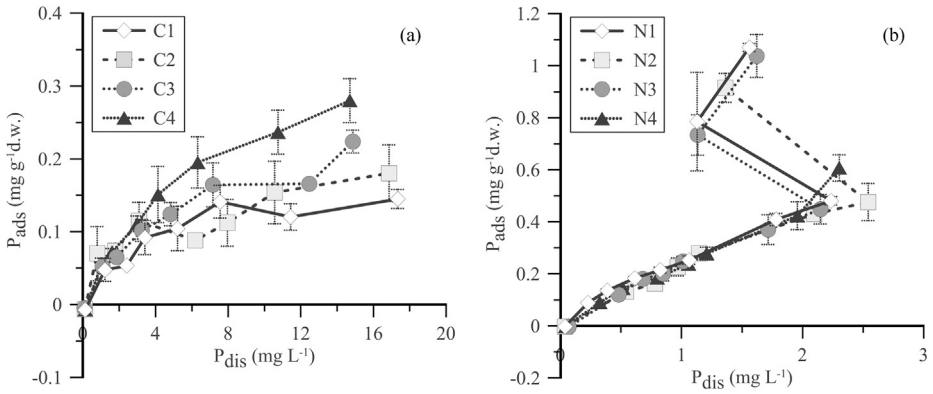

Fig. 4. Isotherms experiments in sediments of (a) El Carrizal Reservoir (ECR) and (b) El Nihuil Reservoir (ENR). P_{ads}: P adsorbed to sediment after 48 h., P_{dis}: P concentration remaining in solution after 48 h. Error bars indicate one standard deviation (n = 3).

organic matter content. Sediment pH was found to be correlated to both P content and sorption behavior since the more alkaline samples had the lesser TP, Fe/Al-P, NAP, and P_{max}. The more abundant fractions, Fe/Al-P and Ca-P, were directly correlated to TP suggesting a higher contribution of the former over the latter. The NAP content and P_{max} were directly correlated to LOI and TP and also to labile-P and Fe/Al-P suggesting a link between these fractions and adsorption phenomenon.

Principal components analysis (Fig. 5) was done considering only those variables whose average values differed between reservoirs. The first two axes accounted for 93.0% of the data variability and clearly separated the two reservoirs. PC1 explained 80.8% of the variation and was related directly to labile-P, Fe/Al-P, NAP, P_{max}, and TP, and inversely related to pH and org-P.

4. Discussion

Fluvial transport is usually the main source of suspended particulate matter (SPM) in reservoirs (Thornton et al., 1990), and, therefore, basin geomorphology and lithology are key features to consider when analyzing sediment P sources and dynamics. In granitic-and basaltic-dominated catchments, suspended load tends to be much smaller than in basins with significant proportions of sedimentary rocks (Meybeck & Ragu, 1996), and although volcanic and plutonic rocks are abundant in the upper basin of the ECR and ENR, *ca.* 20% of the exposed rocks is comprised of sandstones, conglomerates, shales (Nullo et al., 2005; Ramos et al., 2010); this lithological feature, together with glacier abrasion and sharp intra-annual hydrological variations, causes high solid fluxes yielding *ca.* 77 t km^{-2} y^{-1} at the ECR inflow (León, 2013).

4.1. Physical characteristics of sediments

Grain size influences P transport and bioavailability; clay-sized particles have higher concentrations of P than coarse sediments due to stronger surface interactions occurring in the former (Golterman, 2004). In reservoirs, particle size sorting is controlled by selective settling caused by inflow velocity variation along the longitudinal axis; the coarser and heavier particles (sand) deposit at the river mouth and the smaller and lighter particles (silt and clay) accumulate in deeper areas. Considering a reservoir as a continuum from its tributaries to the dam, it is possible to identify a longitudinal gradient and the following areas can be

Table 4
Linearized Langmuir isotherm (eq. 1) parameters for sediment samples from the El Carrizal Reservoir (ECR) and El Nihuil Reservoir (ENR). P_{max}: maximum P sorption capacity, K_L: binding energy constant, EPC_0: P equilibrium concentration, and NAP: native adsorbed P, P_{des}: desorpted P, *i.e.*-[P_{dis}] in the treatment with no added P. Variables marked with * indicate significant difference between the reservoirs ($p < 0.05$, $n = 4$. Kruskal-Wallis test).

		ECR				ENR			
		C1	**C2**	**C3**	**C4**	**N1**	**N2**	**N3**	**N4**
Fitting parameters	$1/P_{max}$	5.008	4.976	4.275	2.791	1.527	0.716	0.458	0.928
	$1/(K_L \cdot P_{max})$	21.565	17.200	17.420	16.537	3.611	3.611	3.713	3.274
	R^2	0.92	0.87	0.95	0.99	0.99	0.97	0.99	0.99
P_{max}*	(mg g^{-1} d.w.)	0.200	0.201	0.234	0.358	0.579	1.343	2.181	1.077
K_L	(L mg^{-1})	4.3	3.5	4.1	5.9	1.3	4.8	8.1	3.5
EPC_0	(mg L^{-1})	0.082	0.107	0.080	0.195	0.036	0.053	0.082	0.048
NAP*	(mg g^{-1} d.w.)	0.002	0.004	0.003	0.011	0.014	0.015	0.025	0.015
P_{des}*	(mg g^{-1} d.w.)	0.007	0.006	0.005	0.007	0.002	0.003	0.004	0.003

Table 5
Significant correlations between physical and chemical variables in sediments of the El Carrizal Reservoir and El Nihuil Reservoir ($n = 8$). R_S: Spearman correlation coefficient. See text and Tables 2 and 4 for variables reference.

Variable(1)	**Variable(2)**	**R_S**	**p-value**
Total N	LOI	0.93	0.0140
Total P	pH	-0.84	0.0085
Total P	Fe/A-P	0.79	0.0376
Total P	Ca-P	0.83	0.0275
Labile-P	Fe/A-P	0.98	0.0098
Fe/A-P	pH	-0.77	0.0251
NAP	pH	-0.87	0.0053
NAP	LOI	0.86	0.0068
NAP	Total P	0.79	0.0195
NAP	Labile-P	0.93	0.0007
NAP	Fe/A-P	0.97	0.0001
K_L	Clay	0.79	0.0186
P_{des}	EPC_0	0.86	0.0233
P_{max}	pH	-0.81	0.0154
P_{max}	LOI	0.76	0.0438
P_{max}	Total P	0.83	0.0275
P_{max}	Labile-P	0.93	0.0140
P_{max}	Fe/A-P	0.98	0.0098
P_{max}	NAP	0.97	0.0001

distinguished: riverine, transition, and lacustrine. Each one of these has distinctive physical, chemical and biological properties but differs in P circulation (Bartoszek & Tomaszek, 2011). Nevertheless, in more dynamic reservoirs, this pattern is seldom observed because the sediment transport, resuspension, and redistribution within the reservoir are affected by inflow and outflow pulses (Jørgensen et al., 2013; Morris & Fan 1998; Thornton et al., 1990).Within a hydrological year, the ECR and ENR experience two marked filling/draining stages caused by the combination of the strongly seasonal inflow and the high water withdrawal at low inflow discharge. This hydraulic instability is consistent with the poorly sorted grain-size distribution recorded in both reservoirs.

4.2. Chemical and mineralogical characteristics of sediments

In fluvial sediments, potassium enrichment (K/Al) of the bulk sample is often used as an indicator of chemical alteration since it is considered to be related to K-feldspar and clay weathering (Shao et al., 2012); a lower K/Al ratio assumes K loss indicating higher weathering intensity, and *vice versa* (Buggle et al., 2011). The world average of this ratio in the continental crust has a value close to 0.35 (Viers et al., 2009) while, the values in weathered rocks are close to 0.15 (Lopez et al., 2012). In the sediments of the ECR and ENR, the K/Al ratio was homogeneous and averaged 0.20

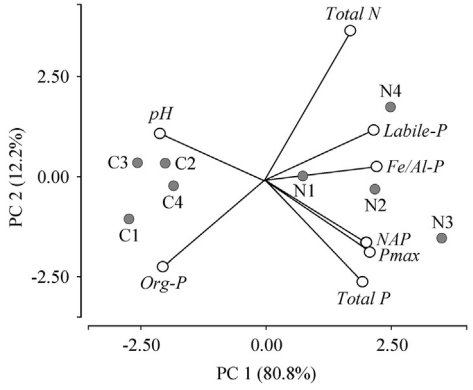

Fig. 5. Principal components analysis biplot of sediment in El Carrizal Reservoir (ECR) and El Nihuil Reservoir (ENR) (**bold**), and physical and chemical variables (*italics*) distribution in the first factorial plane. Only variables differing between reservoirs were considered.

suggesting a moderate chemical alteration of sediments in both reservoirs. Also, the relatively high abundance of readily weatherable minerals in the sediments studied may indicate that neither strong chemical weathering nor early diagenesis has occurred.

In both reservoirs, the elemental composition of sediments reflected the sedimentary lithology of each basin (Nullo et al., 2005; Ramos et al., 2010; Sruoga et al., 2005). The most noticeable feature was the calcium enrichment, which may be attributed to the abundance of limestone and gypsum (León & Pedrozo, 2015). This phenomenon was apparent when analyzing the Ca and Mg enrichment compared to the world average composition of the Earth´s crust and also to river sediments in South America (Fig. 2). Calcium-enrichment was also observed by Lopez et al. (2006) in sediments from Spanish reservoirs in sedimentary basins. The average Ca/Al ratio in sediments from sedimentary catchments determined by those authors was 1.3 (*vs.* 0.04 from siliceous catchments). They established that the weathering and dissolution of Ca-bearing minerals (plagioclase, calcite, gypsum, etc.) produced high water mineralization and sediment calcium enrichment due to Ca-bearing minerals precipitation. The results of this study showed an average 0.5 Ca/Al ratio for both reservoirs which, together with the Ca-rich mineralogical composition observed (Table 3), may indicate that a similar process is controlling this element content in the ECR and ENR sediments.

In rivers draining calcareous lithologies, calcium precipitates are known to account for a significant proportion of the transported suspended particulate matter (Ollivier et al., 2011). In the Tunuyán River, León and Pedrozo (2015) determined that *ca.* 10% of the minerals transported as suspended particulate matter correspond to calcium salts, and an equal amount is expected in the

Atuel River (main ENR tributary) given the lithological and hydrological similarities between these hydrographic catchments. Mineralogical results showed that calcium salts are abundant in both reservoirs and that the greatest proportion corresponded to calcium phosphates. It is noteworthy that the higher proportion of these minerals in reservoir sediments with respect to river suspended material (18% *vs.* 10%), which suggests in-reservoir calcium precipitation. Considering these settings, it is expected that the calcium phosphates sources in the sediments of the ECR and ENR would be both allochthonous and autochthonous, as phosphates are abundant in marine sedimentary rocks (Boggs, 2009) such as those eroded from the basins studied (Nullo et al., 2005; Ramos et al., 2010; Sruoga et al., 2005), and they also co-precipitate with Ca^{2+} in surfaces of ironoxy(hydr)oxides, aluminum hydroxides, clays, and calcite (House, 1990). Given that these compounds are quite insoluble in the pH range of natural waters (6.5–8.3), they are expected to act more as a sink rather than as a source of P.

The content of iron(oxy)hydroxides and aluminum hydroxides in sediments is known to influence P dynamics through surface binding to hydrated species in colloidal form and into fine particles coated by it (Golterman, 2004). Lopez et al. (2006) found that the Fe/Al ratio in the surface sediment is indicative of endogenous precipitation of iron oxides, and this appears to be closely associated with the sedimentary phosphorus accumulation above the baseline. These authors found a constant average value of 0.2 for all reservoirs sampled, which is small when compared to the 0.5 average registered in both the ECR and ENR, suggesting that iron content may be a significant factor controlling P mobility in these reservoirs.

Another factor affecting P dynamics in sediment is submerged vegetation (macrophytes), which may have a significant effect on the nutrients circulation in a water body acting as a potential nutrient pump (Casbeer, 2009). In general, aquatic vegetation can be considered a sink of P during its growth period and a source of P during senescence stage (Carpenter & Lodge, 1986). The riverine zones of the ECR and ENR are morphometrically different being relatively narrow and deep in the former, and shallow and wide in the latter. These features produce a highly turbid environment in the ECR and a well-illuminated water column in the ENR, resulting in low and high planktonic productivity, respectively. Also, light availability in this part of ENR allows a dense *Chara* sp. cover, which is known to thrive in low light conditions (Van den Berg et al., 1998) and to produce calcium deposition in its stems (Daily, 1975), which may explain the higher Ca proportion recorded at site N1 (Table 2). Furthermore, given its morphometric features (Z_{avg} = 3 m), the higher organic content in the ENR is expected to be linked to the intense sediment-water interaction and the impact of aquatic vegetation (Scheffer, 2004).

The TC and TN contents in both reservoirs (3–4% and 0.1–0.3%, respectively) were comparable to those unpolluted sediments (Golterman, 2004) and were similar to those in Alicura (3% and 0.4%), a low productivity reservoir in a granitic basin in Patagonia (Temporetti & Pedrozo, 2000). Also, the LOI proportion in the ECR (5.1%) and the ENR (7.3%) resembled more to low productivity reservoirs than to eutrophic systems such as the San Roque Reservoir (LOI = 13%), located in a heavily modified basin in central Argentina (Borgnino et al., 2006a). In both reservoirs sampled, the LOI also seemed to be linked to phytoplankton productivity since a higher value was recorded at site S2 (6.2%) along with higher chlorophyll-***a*** concentration (León et al., 2016); the LOI values in the ENR were also higher at sites with higher limnetic development.

4.3. Phosphorus content and fractionation

Although P content in reservoir sediments is considered to be higher than in lakes (Thornton et al., 1990), TP in reservoirs in sedimentary basins may be expected to be even higher because of the direct relationship between P and solids load (Golterman, 2004; Huang et al., 2015). Furthermore, the higher intensity of physical factors operating in mountain catchments is likely to synergize with lithology causing an increase in particulate matter flux (León & Pedrozo, 2015). The sedimentary formations in the upstream ECR and ENR catchments are comprised of interspersed layers of marine and continental deposits containing P-rich minerals in shales, limestone, and evaporites (Boggs, 2009). Accordingly, TP concentration in ECR and ENR sediments (1.1 and 1.6 mg g^{-1} d.w., respectively) was observed to be higher than in coastal sediments (0.5–0.7 mg g^{-1} d.w., [Cong et al., 2014]) and reservoirs of granitic basins (0.2–0.6 mg g^{-1} d.w., [Temporetti & Pedrozo, 2000]), and it is comparable to other Andean sedimentary catchments (1.3 mg g^{-1} d.w., [Pedrozo & Bonetto, 1987]). The average TP concentration in suspended particulate matter in the Tunuyán River upstream pollution sources (1.1 mg g^{-1} d.w., [León, 2013]) was comparable to that in the ECR sediments; therefore, it is likely that TP in the reservoir sediments is not significantly affected by human activities.

In aquatic environments, P solubility is considered a measure of its biological availability and it depends on water and sediment chemical compositions, as well as on physical and biological conditions at the water-sediment interface (Boström et al., 1988; Lu et al., 2016). In order to assess the chemical distribution of P in sediments, chemical fractionation studies are commonly used (Lukkari et al., 2007), which allow further estimation of its mobility and its role in the eutrophication process. As observed by Cong et al. (2014) for coastal sediments, the largest fraction in the ECR and ENR sediments was Ca-P as expected considering the calcium-enriched lithology of both basins, in which P is mostly associated to authigenic carbonate-apatite (Filipelli, 2008). In agreement with that P binding mechanism, the more abundant Ca-bearing phosphates recorded in the ECR and ENR mineralogical composition were monetite (6%) and brushite (2%), both precursors of apatites (Sposito, 2008).

Spatial distribution of Fe/Al-P and Ca-P observed in the ECR and ENR coincided with the pattern described by Borgnino et al. (2006b) in which the former fraction is higher in the deeper areas of finer sediments, and the latter is more abundant in the riverine zone together with coarser particles. The sediment clay fraction has greater specific surface area which supports higher concentration of Fe/Al-P (Borgnino et al., 2006b). This relation was not clear in either the ECR or ENR probably due to the combination of hypolimnetic anoxia acting on Fe/Al-P in the ECR (see next section) and to macrophyte uptake in ENR (Gao et al., 2009). A close and positive relation between labile-P and NAP was found in both reservoirs, which is consistent with labile-P being the most readily bioavailable fraction given its loose binding to sediments (Lin et al., 2009). The proportions of labile-P in the sediments studied (2–5% of TP) were comparable to those in calcareous water lakes (Dittrich et al., 2013; Hupfer et al., 2009).

In the ECR and ENR, hydrology and reservoir morphometry may play an important role in P fraction dynamics as the seasonality of discharge causes marked intra-annual variations in water flux and composition (León & Pedrozo, 2015; León et al., 2016; Peralta & León, 2006). The shallow water column in the ENR compared to that in the ECR should have significant effects on the reservoir physical dynamics and the sediment distribution. Also, the physical conditions in the overlying water differ between the reservoirs; the ECR thermally stratifies during summer diminishing hypolimnetic dissolved oxygen concentration (León et al.,

2016), while for the ENR the shallow water column and strong winds prevent stratification and generate a continuously oxygenated bottom (Peralta & León, 2006). Redox potential in oxic and alkaline environments (as in the ENR) should be higher than that in anoxic and circumneutral conditions (as in the ECR), promoting higher concentrations of labile-P and Fe/Al-P, the redox-sensitive fractions (Sposito, 2008). Also, in the anoxic hypolimnion of eutrophic lakes, a high dissolved sulfate concentration results in sulfide production promoting the release of iron bound P from sediments (Chen et al., 2016; Smolders et al., 2006). These phenomena may explain the higher contents of Fe/Al-P in the oxygenated bottom of the ENR compared to those in the anoxic hypolimnion of the summer-stratifying ECR (León et al., 2016). Further evidence of the effect of the water sulfate content on the ECR sediments biogeochemistry is the occurrence of a tenfold increase in the hypolimnetic concentrations of ammonia during stratification *vs*. mixing periods (*ca*. 20 up to 200 $\mu g\ N\ L^{-1}$) coupled with marked decreases in nitrate concentration (León, 2013). This scenario agrees with the stimulation of dissimilatory nitrate reduction to ammonia (An & Gardner, 2002), which has been indicated to result from water sulfate enrichment producing sulfide in anoxia, with the latter the factor inhibiting denitrification (Baldwin & Mitchell, 2012).

Organic-P was the second most significant P system in the ECR while the ENR showed lesser concentrations. This fraction is often called residual P because it includes both organic and refractory P (Hupfer et al., 2009; Psenner & Pucsko 1988). Golterman (2004) pointed out that this fraction is mostly comprised of dead phytoplankton, which is consistent with the ECR water column being phytoplankton-dominated while in the ENR the presence of macrophytes keeps the microalgae abundance low (Wetzel, 2001).

The sediment grain size and elemental and mineralogical compositions did not differ between the reservoirs, while pH did. Sediments in the ECR were more alkaline and, accordingly, labile-P and Fe/Al-P fractions were likely to be adversely affected by pH, showing lower concentrations.

4.4. Phosphorus sorption

In order to simplify a complex phenomenon, various assumptions underlie P adsorption experiments. In most cases P_{ads} is estimated from dissolved P disappearance and it is assumed that P leaving solution distributes homogeneously on particle surfaces and conversely fixes to finite sorption sites (Limousin et al., 2007). However, dissolved P concentration in calcareous systems such as the ECR and ENR may also decrease due to co-precipitation with carbonates (House, 1990). The factors controlling which P removal process will dominate (adsorption *vs.* co-precipitation) are temperature, pH, ionic force, contact time, and Ca and P concentrations (Yagi & Fukushi, 2012). In the systems studied these factors are seasonally variable (León & Pedrozo, 2015; León et al., 2016); hence, the direct extrapolation of *in vitro* data to the environmental system should not be linear (Huang et al., 2015; Sposito, 2008).

Isotherm experiments have been used to estimate P adsorption in soils (Tunesi et al., 1999), in sediments of rivers (Lin et al., 2009) and reservoirs (Wang et al., 2009), and in purified solid media (Abdala et al., 2015; Freeman & Rowell, 1981; Perassi & Borgnino, 2014; Yagi & Fukushi, 2012); and it has been consistently found that adsorption dominates at low dissolved P concentrations ($< 3–5\ mg\ L^{-1}$) and co-precipitation with carbonates becomes significant at higher loads ($> 5\ mg\ L^{-1}$). In batch experiments, a typical Langmuir adsorption isotherm was observed only in the ECR, while in the ENR the plot showed a steeper slope which changed from positive to negative. This latter pattern has been established to result from initial adsorption at low dissolved P concentrations and P-carbonate co-precipitation at higher P loads (Freeman & Rowell, 1981; Yagi & Fukushi, 2012). Accordingly, the percentage of P_{dis} after incubation in the ENR was low (18%) compared to that in the ECR (69%) suggesting that P co-precipitation may be occurring in the ENR at higher rates than in ECR. Perassi and Borgnino (2014) observed that in $CaCO_3$–montmorillonite, P co-precipitation increased with humic acids concentration, and since this variable is expected to be higher in ENR due to higher sediment organic content (Table 2), it is likely that the P co-precipitation process dominates in the ENR sediments in contrast to what occurs in the ECR, where P_{dis} concentrations remained in solution even at high P concentrations ($15\ mg\ L^{-1}$) suggesting adsorption prevalence.

Phosphorus adsorption also depends on the net charge on the surface of particles, which is in turn affected by pH through the modification of sorption sites availability via competition of the hydroxyl anion with phosphate (Langmuir, 1997). In this study, P fractionation in the ECR and ENR showed that labile-P and Fe/Al-P in the more alkaline ECR sediments (pH 8.0) were lower ($0.09\ mg\ P\ g^{-1}$d.w.) than in the ENR circumneutral sediments (pH 7.2), where those fractions were found be higher ($0.26\ mg\ P\ g^{-1}$d.w.). This difference may indicate that non-apatite inorganic P distribution in the sediments of these reservoirs is also influenced by pH and ionic contents.

The EPC_0 is considered an indicator of the sediments capacity to act as a source or sink of phosphate (Zhou et al., 2005). If overlying water P concentration is $< EPC_0$, sediments may release P (fixed as NAP) and, in the opposite case, sediments retain P and NAP increases. In the reservoirs studied, the annual average hypolimnetic SRP concentration was always lower than EPC_0, and, although this fact suggests that sediments may be releasing P to the water column, it is worth considering that EPC_0 is a parameter determined *in vitro* and, therefore, chemical variables controlling P release (pH, DO, and redox potential) are expected to differ from those *in situ* due to experimental artifacts; *e.g.* differences in the solid/solution ratio between natural conditions and batch experiments (Limousin et al., 2007). However, evidence suggests that the ECR sediments act as a P source during water column stratification occurring in the summer as hypolimnetic SRP concentrations increases (*ca.* $0.07\ mg\ P\ L^{-1}$) regardless of the inflow SRP concentration being at its annual lowest due to the snowmelt dilution effect (León et al., 2016). In the ENR sediments P release should be less marked because no anoxia occurs at the sediment-water interface due to water column shallowness and the high effective fetch acting upon it (Peralta & León, 2006).

Results suggest that the sediments in both reservoirs may act seasonally as a dissolved P source since labile-P and Fe/Al-P are the main fractions involved in supplying P. Nevertheless, given the magnitude of Ca-P and organic-P fractions in the environments studied, more detailed research about the depth distribution and movement of P is needed in order to elucidate the relative contributions of the different compartments of the P cycle in these calcium- and sulfate- dominated systems.

5. Conclusions

The sediments in both reservoirs showed moderate to low chemical alteration and calcium-enriched composition, because calcium phosphate salts are the most abundant P-bearing mineral. Sediments had higher TP concentrations than concentrations recorded in granitic basins and the TP concentrations are similar to those in sedimentary basins, while TC and TN concentrations were similar to those observed in unpolluted sediments. In both reservoirs, P-Ca was the most abundant fraction and P-Fe/Al was higher in oxic sediments. The calculated Fe/Al ratios and the observed

chemical conditions (high pH and calcium concentration) indicated that sediment Fe content is likely to control P mobility towards the water column in both reservoirs as P-Ca dissolution should not be favored. The high sulfate concentration in the reservoirs' water and the difference in bottom oxygenation conditions between them (stratifying anoxic ECR *vs*. mixed oxic ENR) are likely to control the P release from these reservoirs sediments.

Acknowledgements

We wish to thank C. Menconi, R. Inzirillo and A. Atencio for sampling assistance and L. Simonella for XRD data processing. This study received financial support from Agencia Nacional de Promoción Científica y Tecnológica (PICT 2010-0270) and from Universidad Nacional del Comahue (Program 04/B166). FLP and PFT are members of CONICET. We also thank two anonymous reviewers whose comments improved the original manuscript.

References

Abdala, D. B., Northrup, P. A., Arai, Y., & Sparks, D. L. (2015). Surface loading effects on orthophosphate surface complexation at the goethite/water interface as examined by extended X-ray Absorption Fine Structure (EXAFS) spectroscopy. *Journal of Colloid and Interface Science*, *437*, 297–303.

An, S., & Gardner, W. S. (2002). Dissimilatory nitrate reduction to ammonium (DNRA) as a nitrogen link, versus denitrification as a sink in a shallow estuary (Laguna Madre/Baffin Bay, Texas). *Marine Ecology Progress Series*, *237*, 41–50.

Baffico, G. D., Pedrozo, F., Temporetti, P., & Diaz, M. (2007). *Relationships between macrophytes and their environment in El Nihuil reservoir (Mendoza, Argentina)* (Technical Report). Argentina: S.C. de Bariloche. (In Spanish)

Baldwin, D. S., & Mitchell, A. (2012). Impact of sulfate pollution on anaerobic biogeochemical cycles in a wetland sediment. *Water Research*, *46*(4), 965–974.

Bartoszek, L., & Tomaszek, J. (2011). Analysis of the spatial distribution of phosphorus fractions in the bottom sediments of the Solina–Myczkowce Dam reservoir complex. *Environment Protection Engineering*, *37*(3), 5–15.

Berg, U., Neumann, T., Donnert, D., Nüesch, R., & Stüben, D. (2004). Sediment capping in eutrophic lakes – Efficiency of undisturbed calcite barriers to immobilize phosphorus. *Applied Geochemistry*, *19*, 1759–1771.

Boggs, S. (2009). *Petrology of Sedimentary Rocks*. Cambridge: Cambridge University Press.

Borgnino, L., Avena, M., & De Pauli, C. P. (2006a). Surface properties of sediments from two Argentinean reservoirs and the rate of phosphate release. *Water Research*, *40*, 2659–2666.

Borgnino, L., Orona, C., Avena, M., Maine, M. A., Rodriguez, A., & De Pauli, C. P. (2006b). Phosphate concentration and association as revealed by sequential extraction and microprobe analysis: The case of sediments from two Argentinean reservoirs. *Water Resources Research*, *42*, 1–12.

Boström, B., Andersen, J. M., Fleischer, S., & Jansson, M. (1988). Exchange of phosphorus across the sediment-water interface In: G. Persson, & M. Jansson (Eds.), *Phosphorus in Freshwater Ecosystems* (pp. 229–244). Dordrecht: Springer.

Buggle, B., Glaser, B., Hambach, U., Gerasimenko, N., & Marković, S. (2011). An evaluation of geochemical weathering indices in loess–paleosol studies. *Quaternary International*, *240*(1), 12–21.

Carpenter, S. R., & Lodge, D. M. (1986). Effects of submersed macrophytes on ecosystem processes. *Aquatic Botany*, *26*, 341–370.

Carter, M. R., & Gregorich, E. G. (Eds.). (2006). *Soil Sampling and Methods of Analysis*. Boca Raton: CRC Press.

Casbeer, W. C. (2009). *Phosphorus fractionation and distribution across delta of deer creek reservoir* (Master of Science Thesis). Provo, VT: Brigham Young University.

Chen, M., Li, X. H., He, Y. H., Song, N., Cai, H. Y., Wang, C., & Jiang, H. L. (2016). Increasing sulfate concentrations result in higher sulfide production and phosphorus mobilization in a shallow eutrophic freshwater lake. *Water Research*, *96*, 94–104.

Cong, M., Jiang, T., Qi, Y. Z., Dong, H. P., Teng, D. Q., & Lu, S. H. (2014). Phosphorus forms and distribution in Zhejiang coastal sediment in the East China Sea. *International Journal of Sediment Research*, *29*(2), 278–284.

Daily, F. K. (1975). A note concerning calcium carbonate deposits in charophytes. *Phycologia*, *14*(4), 331–332.

Di Rienzo, J. A., Casanoves, F., Balzarini, M. G., González, L., Tablada, M., & Robledo, C. W. (2013). *InfoStat Versión 2013. Córdoba*. Argentina: FCA, Universidad Nacional de Córdoba.

Dittrich, M., Chesnyuk, A., Gudimov, A., McCulloch, J., Quazi, S., Young, J., & Arhonditsis, G. (2013). Phosphorus retention in a mesotrophic lake under transient loading conditions: Insights from a sediment phosphorus binding form study. *Water Research*, *47*(3), 1433–1447.

EVARSA (2006). *Study on Siltation in El Carrizal Reservoir Province of Mendoza* (Technical report (final). Mendoza, Argentina: Evaluación de Recursos S.A. (In Spanish)

EVARSA (2013). *Study on Siltation in El Carrizal Reservoir Province of Mendoza* (Technical report (final). Mendoza, Argentina: Evaluación de Recursos S.A. (In Spanish)

Filipelli, G. M. (2008). The global phosphorus cycle: Past, present, and future. *Elements*, *4*, 89–95.

Freeman, J. S., & Rowell, D. L. (1981). The adsorption and precipitation of phosphate onto calcite. *Journal of Soil Science*, *32*(1), 75–84.

Gao, Y. X., Zhu, G. W., Qin, B. Q., Pang, Y., Gong, Z. J., & Zhang, Y. L. (2009). Effect of ecological engineering on the nutrient content of surface sediments in Lake Taihu, China. *Ecological Engineering*, *35*(11), 1624–1630.

Golterman, H. L. (2004). *The Chemistry of Phosphate and Nitrogen Compounds in Sediments*. London: Kluwer Academic Publichers.

Hieltjes, A. H., & Lijklema, L. (1980). Fractionation of inorganic phosphates in calcareous sediments. *Journal of Environmental Quality*, *9*(3), 405–407.

House, W. A. (1990). The prediction of phosphate coprecipitation with calcite in freshwaters. *Water Research*, *24*(8), 1017–1023.

Huang, L., Fang, H., Fazeli, M., Chen, Y., He, G., & Chen, D. (2015). Mobility of phosphorus induced by sediment resuspension in the Three Gorges Reservoir by flume experiment. *Chemosphere*, *134*, 374–379.

Hupfer, M., Zak, D., Roßberg, R., Herzog, C., & Pöthig, R. (2009). Evaluation of a well-established sequential phosphorus fractionation technique for use in calcite-rich lake sediments: Identification and prevention of artifacts due to apatite formation. *Limnology and Oceanography: Methods*, *7*(6), 399–410.

Jørgensen, S. E., Tundisi, J. G., & Tundisi, T. M. (2013). *Handbook of Inland Aquatic Ecosystem Management*. Boca Raton: CRC Press.

Kay, S. M., Mpodozis, C., & Ramos, V. A. (2004). Andes In: R. C. Selley, L. R. Cocks, & I. R. Plimer (Eds.), *Encyclopedia of Geology*, 1 (pp. 118–131). Oxford: Elsevier.

Keitel, J., Zak, D., & Hupfer, M. (2016). Water level fluctuations in a tropical reservoir: The impact of sediment drying, aquatic macrophyte dieback, and oxygen availability on phosphorus mobilization. *Environmental Science and Pollution Research*, *23*(7), 6883–6894.

Langmuir, D. (1997). *Aqueous environmental geochemistry*. Upper Saddle River, NJ: Prentice Hall.

León, J. G. (2013). *Nutrient dynamics effect on phytoplankton in embalse El Carrizal, Mendoza, Argentina: Relationship with water quality and use* (Doctoral dissertation). Córdoba, Argentina: National University of Córdoba. (In Spanish)

León, J. G., Beamud, S. G., Temporetti, P. F., Atencio, A. G., Diaz, M. M., & Pedrozo, F. L. (2016). Stratification and residence time as factors controlling the seasonal variation and the vertical distribution of chlorophyll-**a** in a subtropical irrigation reservoir. *International Review of Hydrobiology*, *101*, 1–12.

León, J. G., & Pedrozo, F. L. (2015). Lithological and hydrological controls on water composition: Evaporite dissolution and glacial weathering in the south central Andes of Argentina (33°–34°S). *Hydrological Processes*, *29*, 1156–1172.

Limousin, G., Gaudet, J. P., Charlet, L., Szenknect, S., Barthes, V., & Krimissa, M. (2007). Sorption isotherms: A review on physical bases, modeling and measurement. *Applied Geochemistry*, *22*(2), 249–275.

Lin, C., Wang, Z., He, M., Li, Y., Liu, R., & Yang, Z. (2009). Phosphorus sorption and fraction characteristics in the upper, middle and low reach sediments of the Daliao river systems, China. *Journal of Hazardous Materials*, *170*(1), 278–285.

Lopez, P., Dolz, J., Arbat, M., & Armengol, J. (2012). Physical and chemical characterisation of superficial sediment of the Ribarroja Reservoir (River Ebro, NE Spain). *Limnetica*, *31*, 327–340.

Lopez, P., Navarro, E., Marce, R., Ordoñez, J., Caputo, L., & Armengol, J. (2006). Elemental ratios in sediments as indicators of ecological processes in spanish reservoirs. *Limnetica*, *25*(1-2), 499–512.

Lu, D., Guo, P., Ji, J., Liu, L., & Yang, P. (2016). Evaluation of phosphorus distribution and bioavailability in sediments of a subtropical wetland reserve in southeast China. *Ecological Indicators*, *66*, 556–563.

Lukkari, K., Hartikainen, H., & Leivuori, M. (2007). Fractionation of sediment phosphorus revisited. I: Fractionation steps and their biogeochemical basis. *Limnology and Oceanography: Methods*, *5*(12), 433–444.

Manzur, A., León, J. G., Peralta, P. I., Romay, C., Basile, J. C., Lorenzo, F. E., & Pereira, R. (2006). *Studies on characterization of the Surface Hydric System of Mendoza Province* (Technical report (final). Argentina: Departamento General de Irrigación, PROSAP-OEI: Mendoza. (In Spanish)

Masiokas, M. H., Villalba, R., Luckman, B. H., & Mauget, S. (2010). Intra-to multidecadal variations of snowpack and streamflow records in the Andes of Chile and Argentina between 30 and 37 S. *Journal of Hydrometeorology*, *11*(3), 822–831.

Meybeck, M., & Ragu, A. (1996). *River discharges to the oceans. An assessment of suspended solids, major ions, and nutrients. Environment information and assessment report*. Rpt. Nairobi: United Nations Environment Program.

Morris, G. L., & Fan, J. (1998). *Reservoir sedimentation handbook*. New York: McGraw-Hill Book Co.

Murphy, J., & Riley, J. P. (1962). A modified single solution method for the determination of phosphate in natural waters. *Analytica Chimica Acta*, *27*, 31–35.

Nullo, F. E., Stephens, G., Combina, A., Dimieri, L., Baldauf, P., Bouza, P., & Zanettini, J. C. M. (2005). *Geologic Sheet 3569-III/3572-IV Malargüe, Province of Mendoza (1: 250.000). Buenos Aires: Servicio Geológico Minero Argentino*. Instituto de Geología y Recursos Minerales. (In Spanish)

Ollivier, P., Radakovitch, O., & Hamelin, B. (2011). Major and trace element partition and fluxes in the Rhône River. *Chemical Geology*, *285*(1), 15–31.

Pedrozo, F., & Bonetto, C. (1987). Nitrogen and phosphorus transport in the Bermejo River (South America). *Revue d'Hydrobiologie Tropicale*, *20*(2), 91–99.
Peralta, P., & León, J. (2006). *Studies on limnological characterization of reservoirs in Mendoza Province* (Technical report). Mendoza, Argentina: Departamento General de Irrigación, PROSAP-OEI. (In Spanish)
Perassi, I., & Borgnino, L. (2014). Adsorption and surface precipitation of phosphate onto $CaCO_3$–montmorillonite: Effect of pH, ionic strength and competition with humic acid. *Geoderma*, *232*, 600–608.
Psenner, R., & Pucsko, R. (1988). Phosphorus fractionation: Advantages and limits of the method for the study of sediment P origins and interactions. *Archiv für Hydrobiologie–BeiheftErgebnisse der Limnologie*, *30*, 43–59.
Ramos, V. A., Aguirre Urreta, M. B., Alvarez, P. P., Coluccia, A., Giambiagi, L. B., Pérez, D., & Tunik Vujovich, G. (2010). *Geologic Sheet 3369-III Cerro Tupungato (1: 250.000). Buenos Aires: Servicio Geológico Minero Argentino*. Instituto de Geología y Recursos Minerales. (In Spanish)
Sahuquillo, A., Lopez-Sanchez, J. F., Rauret, G., Ure, A. M., Muntau, H., & Quevauviller, P. (2002). Sequential extraction procedures for sediment analysis In: P. Quevauviller (Ed.), *Methodologies for Soil and Sediment Fractionation Studies* (pp. 10–27). Cambridge: The Royal Society of Chemistry.
Scheffer, M. (2004). *Ecology of shallow lakes*. Berlin: Kluwer Academic Publishers.
Shao, J., Yang, S., & Li, C. (2012). Chemical indices (CIA and WIP) as proxies for integrated chemical weathering in China: Inferences from analysis of fluvial sediments. *Sedimentary Geology*, *265*, 110–120.
Sinke, J. C. (1992). *Phosphorus Dynamics in the Sediment of a Eutrophic Lake. (Doctoral dissertation)*. Wageningen, the Netherlands: Wageningen University.
Smal, H., Ligęza, S., Baran, S., Wójcikowska-Kapusta, A., & Obroślak, R. (2013). Nitrogen and phosphorus in bottom sediments of two small dam reservoirs. *Polish Journal of Environmental Studies*, *22*(5), 1479–1489.
Smolders, A. J. P., Lamers, L. P. M., Lucassen, E. C. H. E.T., Van der Velde, G., & Roelofs, J. G. M. (2006). Internal eutrophication: How it works and what to do about it—A review. *Chemistry and Ecology*, *22*(2), 93–111.
Sposito, G. (2008). *The chemistry of soils*. Oxford: Oxford University Press.
Sruoga, P., Etcheverría, M., Folguera, A., Repol, D., & Zanettini, J. (2005). *Geologic Sheet 3569-I: Volcán Maipo, province of Mendoza (1: 250.000). Buenos Aires: Servicio Geológico Minero Argentino*. Instituto de Geología y Recursos Minerales. (In Spanish)
Temporetti, P., & Pedrozo, F. (2000). Phosphorus release rates from sediments affected by fishfarming. *Aquaculture Research*, *31*, 447–455.
Temporetti, P., Snodgrass, K., & Pedrozo, P. (2013). Dynamics of phosphorus in sediments of a naturally acidic lake. *International Journal of Sediment Research*, *28*(1), 90–102.
Thornton, K. W., Kimmel, B. L., & Payne, F. E. (1990). *Reservoir limnology: ecological perspectives*. New York: John Wiley & Sons.
Tunesi, S., Poggi, V., & Gessa, C. (1999). Phosphate adsorption and precipitation in calcareous soils: The role of calcium ions in solution and carbonate minerals. *Nutrient Cycling in Agroecosystems*, *53*(3), 219–227.
Van den Berg, M. S., Coops, H., Simons, J., & de Keizer, A. (1998). Competition between Chara aspera and Potamogeton pectinatus as a function of temperature and light. *Aquatic Botany*, *60*(3), 241–250.
Viers, J., Dupré, B., & Gaillardet, J. (2009). Chemical composition of suspended sediments in World Rivers: New insights from a new database. *Science of the Total Environment*, *407*(2), 853–868.
Wang, S., Jin, X., Bu, Q., Zhou, X., & Wu, F. (2006). Effects of particle size, organic matter and ionic strength on the phosphate sorption in different trophic lake sediments. *Journal of Hazardous Materials*, *128*, 95–105.
Wang, Y., Shen, Z., Niu, J., & Liu, R. (2009). Adsorption of phosphorus on sediments from the Three-Gorges Reservoir (China) and the relation with sediment compositions. *Journal of Hazardous Materials*, *162*(1), 92–98.
Wetzel, R. G. (2001). *Limnology: Lake and river ecosystems*. San Diego: Academic Press.
Yagi, S., & Fukushi, K. (2012). Removal of phosphate from solution by adsorption and precipitation of calcium phosphate onto monohydrocalcite. *Journal of colloid and Interface Science*, *384*(1), 128–136.
Yu, F., Zou, J., Hua, Y., Zhang, S., Liu, G., & Zhu, D. (2015). Transformation of external sulphate and its effect on phosphorus mobilization in Lake Moshui, Wuhan, China. *Chemosphere*, *138*, 398–404.
Zhou, A., Tang, H., & Wang, D. (2005). Phosphorus adsorption on natural sediments: Modeling and effects of pH and sediment composition. *Water Research*, *39*(7), 1245–1254.